Induction of M-MDSCs with IL6/GM-CSF from adherence monocytes and inhibition by WP1066

HAO HU[1*], YUAN XIANG[2*], TING LI[1*], QI-YING YU[1], LI-XING GU[1], XING-HUA LIAO[1] and TONG-CUN ZHANG[1]

[1]College of Life and Health Sciences, Institute of Biology and Medicine, Wuhan University of Science and Technology, Wuhan, Hubei 430000; [2]Department of Medical Laboratory, Central Hospital of Wuhan, Tongji Medical College, Huazhong University of Science and Technology, Wuhan, Hubei 430014, P.R. China

Received April 1, 2022; Accepted May 19, 2022

DOI: 10.3892/etm.2022.11414

Abstract. Peripheral blood monocytes acquire the phenotype of myeloid-derived suppressor cells (MDSCs) by induction of cytokine or co-culture with cancer cells and are widely used to model MDSCs for *in vitro* studies. However, the simplest method of plastic adhesive sorting is poorly described as the purity of monocyte resulting from this method is the lowest compared with flow cytometry cell-sorting and magnetic beads sorting. Therefore, the present study aimed at investigating the effect of the plastic adhesive monocyte isolation techniques on the resulting MDSCs phenotype. Monocytes were allowed to adhere for 1 h and cultured with IL6 and granulocyte-macrophage colony-stimulating factors (GM-CSF) for 7 days. Plastic adhesion sorting resulted in early low monocyte yield and purity, but high purity of MDSCs was obtained by refreshing the induction medium. The resulting MDSCs were the major subpopulation of $CD33^+CD11b^+CD14^+CD15^-$human leukocyte antigen $(HLA)^{-/low}$ cells and provided the potent capacity to suppress T cell proliferation and cytokine IFN-γ production. Moreover, the induced MDSCs were inhibited by STAT3 inhibitor WP1066, resulting in downregulation of phosphorylated-STAT3 and PD-L1 expression and upregulation of apoptosis respectively. In conclusion, the present study described the generation of monocytic MDSCs from adherence monocytes and the inhibition of STAT3 inhibitor WP1066 on the induced MDSCs. The present study contributed to the development of a new clinical drug, WP1066 targeting MDSC.

Correspondence to: Mr. Xing-Hua Liao or Professor Tong-Cun Zhang, College of Life and Health Sciences, Institute of Biology and Medicine, Wuhan University of Science and Technology, 2 Huangjiahu West Road, Qingling Street, Hongshan, Wuhan, Hubei 430000, P.R. China
E-mail: xinghualiao@wust.edu.cn
E-mail: zhangtongcun@wust.edu.cn

*Contributed equally

Key words: adherence monocytes, myeloid-derived suppressor cells, IL6, granulocyte-macrophage colony-stimulating factors, STAT3 inhibitor WP1066

Introduction

Myeloid-derived suppressor cells (MDSCs) are heterogeneous, immature cell populations of myeloid origin including monocyte/macrophage, granulocyte and dendritic cells, which are one of the major components of the tumor microenvironment protecting cancer cells from the host immune system attack (1-3). MDSCs promote tumor growth by producing immunosuppressive molecules in the TME such as interleukin-10 (4), transforming growth factor-β (5) and reactive oxygen species, as well as expressing cell surface receptors that inhibit T cell proliferation and activation and producing molecules that directly promote tumor growth and invasions such as vascular endothelial growth factor (6) and matrix metalloproteinases (7). There are two major subsets of MDSCs, identified in both mice and humans: Monocytic MDSCs (M-MDSCs) are morphologically and phenotypically similar to monocytes whereas polymorphonuclear MDSCs (PMN-MDSCs) are similar to neutrophils. In mice, M-MDSCs and PMN-MDSCs are defined as $CD11b^+Ly6G^-Ly6C^{high}$ cells and $CD11b^+Ly6G^+Ly6C^{low}$ cells, respectively (8). In humans, M-MDSCs and PMN-MDSCs are defined as $CD11b^+CD14^+CD15^-CD33^+HLA\text{-}DR^{-/low}$ cells and $CD11b^+CD14^-CD15^+CD33^+$ cells, respectively (9,10). It is reported that MDSCs accumulate in patients with renal cell carcinoma (9,11), breast cancer (12,13), ovarian cancer (14,15), melanoma (16) and head and neck cancer (17,18). In some clinical studies, MDSCs are therapeutic targets alone (19-21) or combined with other target drugs such as PD-1/PD-L1 and CTLA-4 immune checkpoint inhibitors (22-24).

In *in vitro* MDSCs studies, there are some different methods to generate MDSCs in mice and humans. One of the major methods is that mouse primary bone marrow cells or human peripheral blood mononuclear cells are co-cultured with mouse or human tumor cell lines or cytokines and then purified by magnetic beads or flow sorting with the use of myeloid cell surface markers such as CD33, CD11b or CD14 (25-29). Another major method is to first obtain high purity myeloid cells, such as monocytes, by magnetic beads

or flow sorting and then co-culturing with tumor cell lines or cytokines. Taking a reductionist approach, the combination of GM-CSF and IL6 could induce normal peripheral blood mononuclear cells (PBMCs) to become $CD33^{+}$ $HLA\text{-}DR^{-/low}$ MDSCs more consistent and potency than combinations of tumor cell-secreted cytokines (30). The present study hypothesized that an obvious limitation of the studies isolating induced MDSCs or freshly monocytes by magnetic beads or flow sorting is the high cost of magnetic bead sorting kits or flow cytometers with sorting function. To overcome this problem, the present study showed that MDSCs were induced from monocytes by plastic adhesive sorting with the cytokine combination of IL6 and GM-CSF. This new model could significantly simplify the manufacturing process of MDSCs and promote drug discovery with MDSCs.

Materials and methods

Isolation of PBMCs. Peripheral blood mononuclear cells (PBMCs) were isolated from anonymous healthy donors. Briefly, the buffy coats were diluted 1:1 in 0.9% NaCl, then centrifuged at 400 x g for 30 min at room temperature, according to the protocol of density gradient centrifugation (Ficoll-Paque). Following centrifugation, PBMCs on the second layer were harvested and washed twice with 30 ml of cold PBS. All human blood samples (150-200 ml) were collected between March 2018 and September 2020 and were performed under the guidelines of the Medical Ethics Committee of the Affiliated Tianyou Hospital, College of Life and Health Sciences, Wuhan University of Science and Technology. (institutional review board approval: WUSTLL-20180009). Each patient involved in the study was asked to sign a written informed consent form and agreed to the use of their samples in scientific research. All the specimens were anonymized and handled according to accepted ethical and legal standards.

Monocytes isolation with plastic adhesion. For monocytes isolation, PBMCs were resuspended in RPMI-1640 medium (Dalian Meilun Biotech Co., Ltd.) supplemented with 10% Fetal Bovine Serum (ExCell Bio. ExCell Biotech Co., Ltd.), seeded in a surface-treated 6-well plate at $2x10^7$ cells/ml in 2 ml. After 1 h of adherence in a 5% CO_2 container at 37˚C, non-adherent cells were removed by washing twice with RPMI-1640 medium and the remaining adherent cells were mostly monocytes.

T cell isolation and activation. For suppression assay, PBMCs isolated from volunteer blood in the above steps were used to sort T cells. According to the instructions (Pan T Cell Isolation kit, human, Miltenyi Biotec GmbH), the PBMCs cell pellet was first resuspended in 40 μl of buffer per 10^7 total cells; second, 10 μl of Pan T Cell Biotin-Antibody Cocktail, 30 μl of buffer and 20 μl of Pan T Cell MicroBead Cocktail was added per 10^7 total cells successively. Then, the LS Column was placed in the magnetic field of a suitable MACS Separator (MidiMACS; Miltenyi Biotec GmbH), the cell suspension added into the column and the flow-through containing unlabeled cells, representing the enriched T cells, was collected. Finally, an appropriate amount of anti-CD3/CD28 magnetic beads was added to activate the T cells (the ratio of magnetic beads to T cells was 2:1).

IL6/GM-CSF induce monocytes to M-MDSCs. For the induction of M-MDSCs, adherent cells were kept cultured in a surface-treated 6-well plate in the complete induction medium [RPMI-1640 with 10% FBS, 10 ng/ml IL6 (PeproTech, Inc.) and 10 ng/ml GM-CSF (PeproTech, Inc.)] for 7 days. The medium was refreshed on day 3 and day 5.

Flow cytometry. Briefly, adherent cells were harvested with 10 min of dissociation with a gentle non-enzymatic cell dissociation reagent Versene (Gibco; Thermo Fisher Scientific, Inc.) followed by gently scraping. Antibody staining was performed in PBS supplemented with 2% FBS for 30 min at 4˚C in the dark. For intracellular antibody staining, cells were treated with the True-Nuclear Transcription Factor Buffer Set. The antibodies used were: CD3 (UCHT1, cat. no. 300458), CD22 (HIB22, cat. no. 302524), CD14 (63D3, cat. no. 367104), CD15 (HI98, cat. no. 301908), CD33 (HIM3-4, cat. no. 303304), CD11b (ICRF44, cat. no. 301324), HLA-DR (TU39, cat. no. 361707), phosphorylated (p)-STAT3 (A16089B, cat. no. 698905), PD-L1 (29E.2A3, cat. no. 329705) (all from BioLegend, Inc.) and two SinoBiological antibodies of Bcl-2 (cat. no. 100126-R204-F), Caspase3 (cat. no. 10050-MM02) and corresponding isotype control. All the antibodies were diluted 1:2.

Suppression assay. The inhibitory function of the induced M-MDSCs were evaluated by their ability to inhibit the proliferation of allogeneic T cells in the following Suppression Assay: T cells were labeled with carboxyfluorescein succinimidyl ester (CFSE; 5 μM; MilliporeSigma) and seeded at $2x10^5$ cells per well in 96-well plates with 100 μl RPMI-1640 medium at 37˚C for 4 days. M-MDSCs from the above cytokine induction cultures were added to T cells at ratios of 1:4. T cell proliferation was provided by anti-CD3/CD28 stimulation beads (Gibco; Thermo Fisher Scientific, Inc.) and IL2 (Beijing T&L Biotechnology Co., Ltd.). Suppression Assay wells were measured by flow cytometry for T cell proliferation after four days. T cells with or without stimulation and activated T cells co-cultured with monocytes were used as controls.

Reverse transcription-quantitative (RT-q) PCR for suppression gene expression. For the suppression gene expression study, monocytes and M-MDSCs were harvested, then total cellular RNA was extracted from $5x10^6$ cells using the RNeasy Mini kits (Qiagen GmbH). RNA (1 μg) was reverse transcribed to cDNA with random hexamer primers using the Transcriptor First Strand cDNA Synthesis kit (Roche Molecular Diagnostics). Afterward, relative cDNA was amplified with gene specific-primers using Hieff qPCR SYBR Green Master Mix (Shanghai Yeasen Biotechnology Co., Ltd.) and run on a Bio-Rad CFX Maestro with PCR cycling conditions: 95˚C 5 min; 95˚C 15 sec; 55˚C 15 sec; and 72˚C 30 sec for 30 cycles. (Bio-Rad Laboratories, Inc.). Data were acquired and analyzed using Bio-Rad CFX Maestro 1.1 software (Bio-Rad Laboratories, Inc.). Gene expression was normalized to the house-keeping gene (GAPDH) and fold change relative to monocytes was determined. Gene specific primers for reverse transcription-quantitative PCR are shown

Table I. Gene specific primers for reverse transcription-quantitative PCR.

Gene	Forward primer (5' à 3')	Reverse primer (5' à 3')
GAPDH	TTAAAAGCAGCCCTGGTGAC	CTCTGCTCCTCCTGTTCGAC
VEGF	CACACAGGATGGCTTGAAG	AGGGCAGAATCATCACGAAG
NOX2	TGCCAGTCTGTCGAAATCTGC	ACTCGGGCATTCACACACC
TGF-β	GCAGAAGTTGGCATGGTAGC	CCCTGGACACCAACTATTGC
PDL1	TATGGTGGTGCCGACTACAA	TGCTTGTCCAGATGACTTCG
ARG1	GTTTCTCAAGCAGACCAGCC	GCTCAAGTGCAGCAAAGAGA
PDL2	ACCGTGAAAGAGCCACTTTG	GCGACCCCATAGATGATTATGC

in Table I. All experiments were performed in at least three independent experiments. RNA extraction, cDNA synthesis, and qPCR were performed according to the manufacturer's protocols.

IFN-γELISA assay. According to the protocol (Human IFN-γ ELISA kit, U-CyTech biosciences), 50 μl of diluted coating antibody solution and 100 μl PBS was added to each well of the ELISA plate, then incubated overnight at 4˚C. Then, 100 μl of diluted standard/blank/samples was added to the wells and the plate sealed and incubated for 2 h at 37˚C. Diluted detection antibody solution (100 μl) was added and incubated for 1 h at 37˚C. Finally 100 μl of diluted SPP conjugate, 100 μl of TMB substrate solution and 100 μl of stop solution was added into each well (resulting in a yellow color) and the plate read at 450 nm within 30 min.

WP1066 treatment on induced M-MDSCs. After 7 days of IL6/GM-CSF induction, M-MDSCs induced *in vitro* were treated with different concentrations of STAT3 inhibitor WP1066 (0, 5 and 10 μM for 24 h and DMSO without WP1066 as a control. Flow cytometry of p-STAT3 expression levels and suppression protein PD-L1 expression was determined. In addition, the toxicity analysis of WP1066 on inducted M-MDSCs was also determined by detecting the level of cell apoptosis and the expression of apoptosis-relative protein Bcl-2 and Caspase3 by flow cytometry.

Statistical analysis. Statistical analysis was performed using GraphPad Prism 5 software (GraphPad Software, Inc.). The results were shown as means ± SEM from at least three independent experiments. Single comparison between two groups was analyzed by Student's t test. Comparisons between multiple groups were determined using ANOVA followed by the Newman-Keuls multiple-comparison test. $P<0.05$ was considered to indicate a statistically significant difference.

Results

The purity of monocytes before and after plastic adhesion. Isolating monocytes from PBMCs and co-culturing with tumor cells or inducing with cytokines is a common way to obtain MDSCs for *in vitro* studies. The present study wanted to explore the effect of monocytes on cell yield, purity and monocyte phenotype using the plastic adhesion isolation method.

Peripheral blood mononuclear cells were isolated from healthy donors by density gradient centrifugation with a median PBMCs count of $720.5x10^6$ cells with a range ($540.0x10^6$ to $790.0x10^6$) and median viability of 96.5% (90.0-97.8). The median monocytes percentage and cell count in PBMC were 11% (9.8-21.6) and $77.6x10^6$ ($50.6x10^6$-$176.8x10^6$) cells respectively. After 1 h of plastic adhesion enrichment, the total number of cells reduced by 76%, with an average of $165.0x10^6$ cells and the median viability was 98.4%. The median percentage of monocytes increased to 21.8% as the number of $34.6x10^6$ on average (Fig. 1A and B). Compare with monocytes separated from flow cytometry, monocytes isolated by plastic adhesion were mixed with a proportion of lymphocytes. However, after 7 days of induction with IL6 and GM-CSF, the mean of the total cells was $23.1x10^6$ and the median percentage of monocytes increased to 94% (82-98%).

The presence of non-monocytes during MDSCs induction. Unlike the high purity of monocytes produced by isolation methods such as flow cytometry cell sorting or magnetic bead sorting, there were numerous non-monocytes such as $CD3^+$ T cells or $CD22^+$ B cells during the MDSCs induction process of the present study. As shown in Fig. 1A and B, the median percentage of $CD3^+$ T cells in 1 h of adherent cells was 52.6% (34.8-68.0%). Meanwhile, median percentage of $CD22^+$ B cells in 1 h of adherent cells was 16.6% (9.7-23.5%); median percentage of $CD3^-CD22^-CD14^-$ cells was 10% (6.8-15.9%). However, after 3 PBS washes and medium changes in the 7 days of the culture process, non-monocytes all decreased to the lowest level ~2-5% (Fig. 1C and D).

The phenotype of MDSCs. Similar to the common definition of human MDSCs (3), the phenotype of *in vitro*-generated MDSCs was evaluated for CD33, CD11b, HLA-DR, CD14 and CD15 expression by flow cytometry in the present study. As described above, human PMN-MDSCs were defined as $CD11b^+CD14^-CD15^+CD33^+$cells and M-MDSCs were defined as $CD11b^+CD14^+CD15^-CD33^+HLA\text{-}DR^{-/low}$ cells. As shown in Fig. 2A, MDSCs show high expression of CD33, CD11b and CD14 and low expression of HLA-DR. However, MDSCs did not show CD15 expression. The results indicated that the method generated only a single subset of $CD11b^+CD14^+CD15^-CD33^+HLA\text{-}DR^{-/low}$ M-MDSCs but no $CD11b^+CD14^-CD15^+CD33^+$ PMN-MDSCs. At the same time, the present study also revealed the changes of above surface marker expression compared with 1 h adherent monocytes (data not shown).

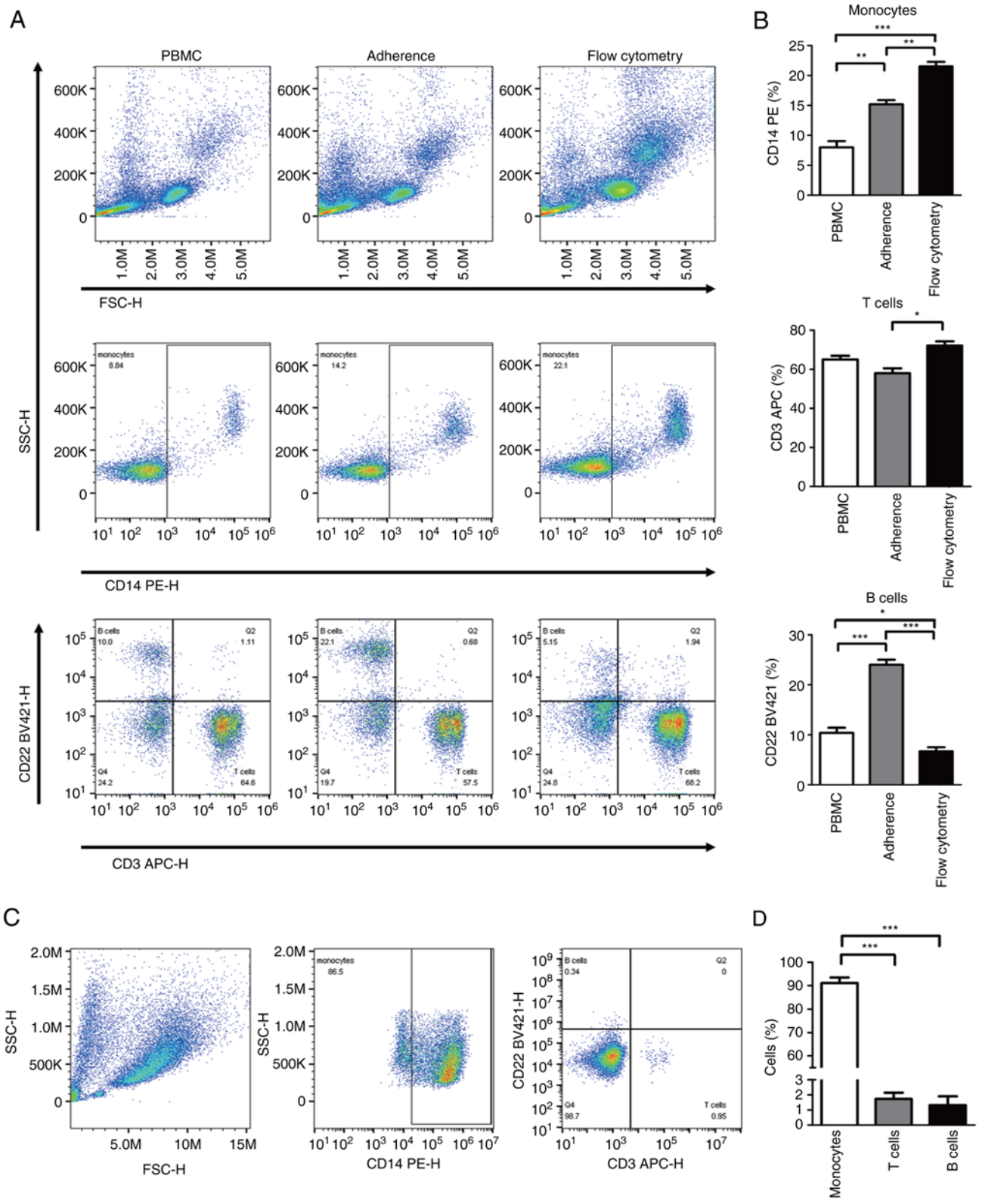

Figure 1. Purity of monocytes before and after plastic adhesion of PBMCs. (A) Streaming representation graph and (B) quantitative analysis of T cells, B cells and monocytes on PBMCs, adherent cells and flow cytometry sorted cells before IL6 and GM-CSF induction. (C) Streaming representation graph and (D) quantitative analysis of T cells, B cells and monocytes after 7 days of IL6 and GM-CSF induction. *P<0.05, **P<0.001, ***P<0.0001. PBMCs, peripheral blood mononuclear cells; GM-CSF, granulocyte-macrophage colony-stimulating factors.

The suppressive ability of MDSCs and suppress gene expression. The inhibitory effect of MDSCs generated from adherent monocytes was evaluated by their ability to inhibit allogeneic T cell proliferation and IFN-γ secretion. As only M-MDSCs were produced, high-purity MDSCs were separated with Versene for 10 min and carefully scraped off the surface of the treated 6-well plate. MDSCs were then mixed with CFSE-labeled allogeneic T cells at MDSCs: T cells ratios of 1:4, followed by stimulation

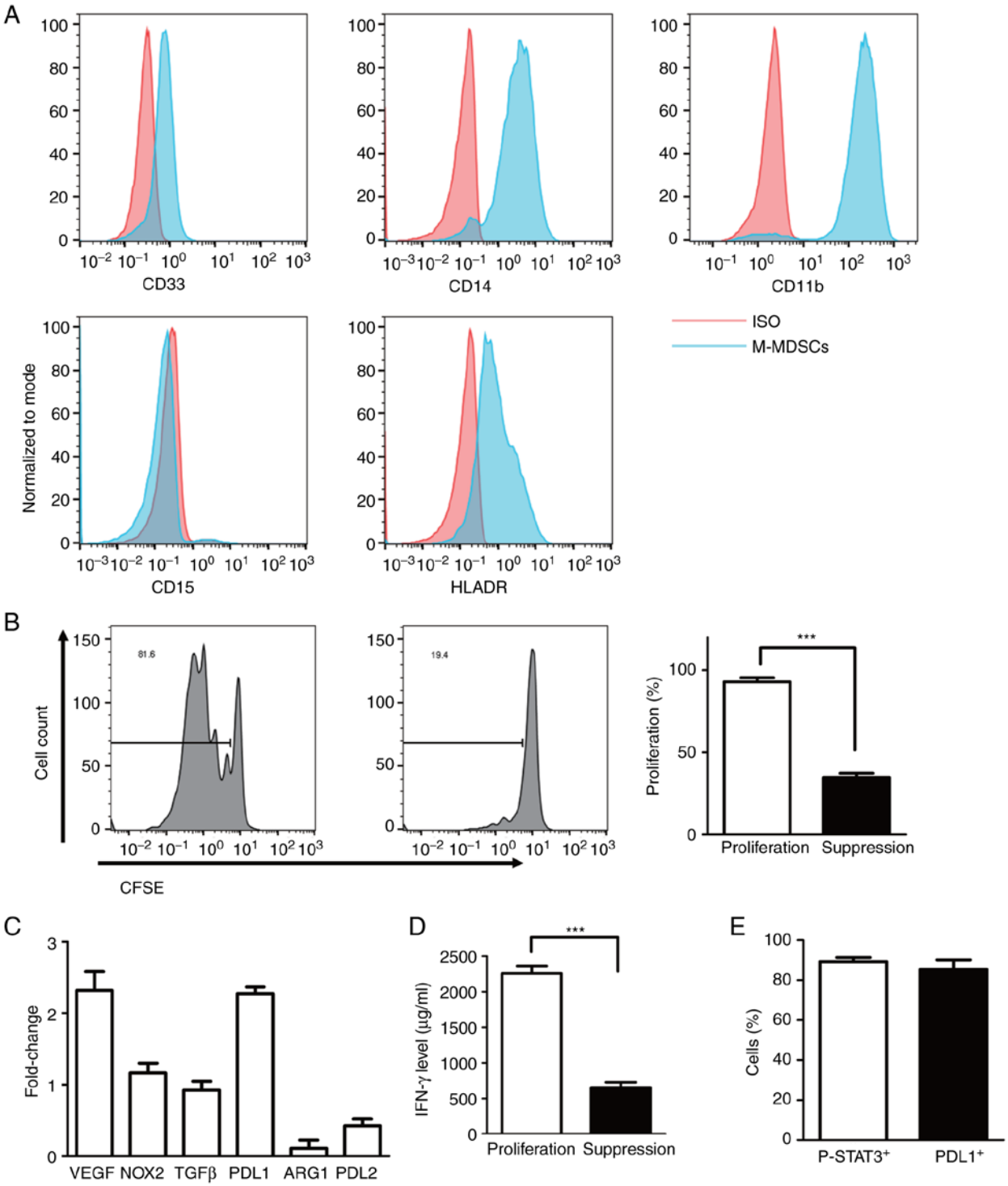

Figure 2. Phenotype of induced MDSCs and suppressing ability. (A) Flow analysis of the cell-surface expression of CD33, CD11b, CD14, CD15 and HLA-DR on *in vitro* induced MDSCs with IL6/GM-CSF for 7 days. (B) and (D) The ability of suppressing T cells proliferation in M-MDSCs at ratio of 1:4 as determined by CFSE label assay and secretion of IFN-γ by ELISA. (C) Gene expression of relative suppressive mechanisms in MDSCs such as VEGF, NOX2, TGF-β, PD-L1, ARG1, PD-L2 in induced M-MDSCs as determined by reverse transcription-quantitative PCR. (E) Percentage of positive p-STAT3 and PDL1 cells in induced M-MDSCs. ***P<0.0001. MDSCs, myeloid-derived suppressor cells; HLA, human leukocyte antigen; GM-CSF, granulocyte-macrophage colony-stimulating factors; M-MDSCs, monocytic MDSCs; CFSE, carboxyfluorescein succinimidyl ester; NOX2, NADPH oxidase 2; PD-L, programmed death ligand; ARG1, arginase 1; p-, phosphorylated.

with anti-CD3/CD28 beads. T cell proliferation was evaluated by flow cytometry after 4 days. Notably, the proliferation of T cells was significantly inhibited with 98% of proliferation T cells with control compared with 36% of proliferation T cells with MDSCs co-culture (Fig. 2B). To reveal the molecular mechanism of suppressing T cell proliferation, some putative suppressor genes including VEGF, ARG1, PD-L1, PD-L2, NOX2 and TGFβ were tested by RT-qPCR. As shown in Fig. 2C, the suppressor genes of PD-L1 and VEGF were shown to be upregulated, which may affect the inhibitory ability of MDSCs.

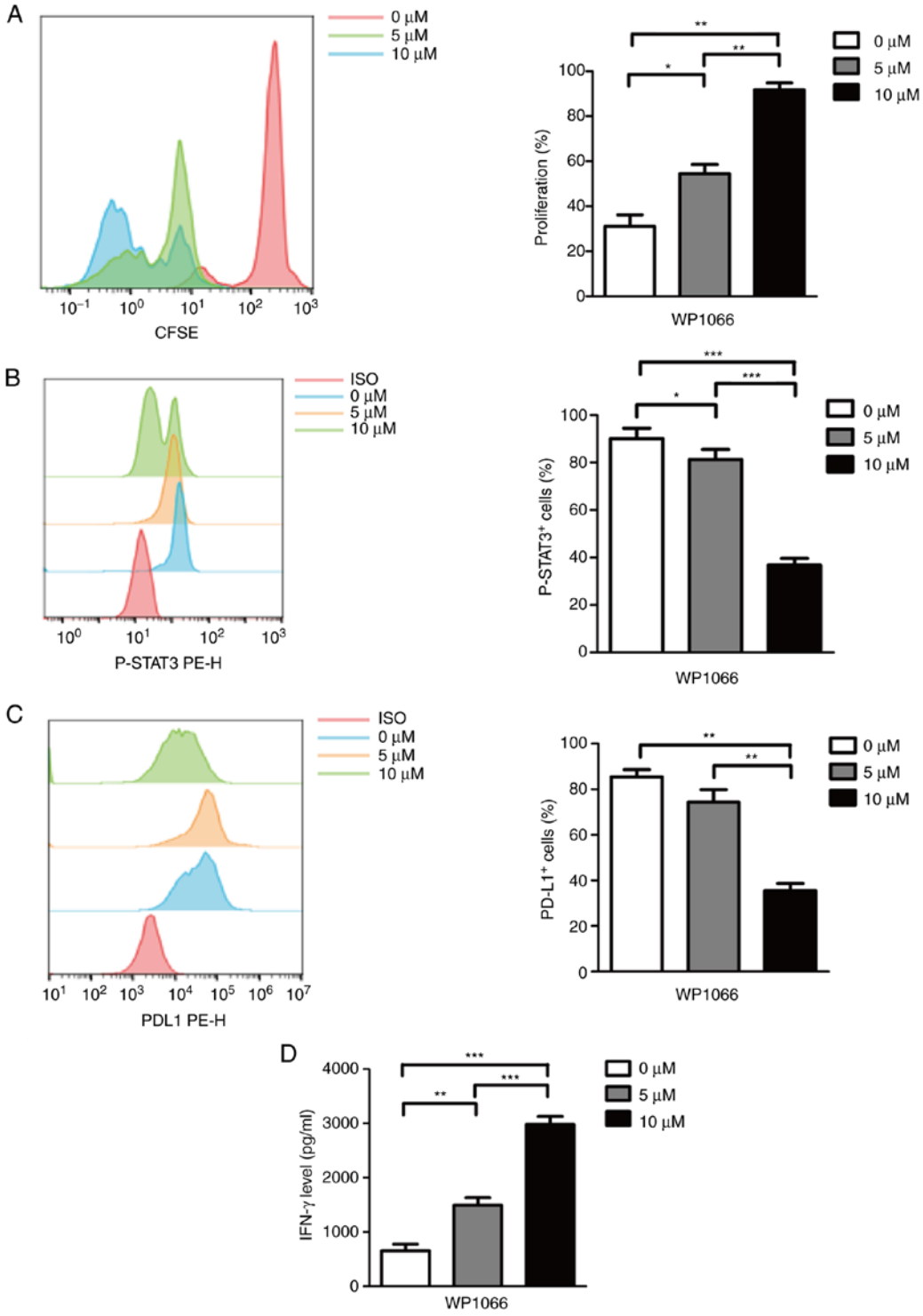

Figure 3. WP1066 treatment leads to downregulation of p-STAT3 and PD-L1. (A) Flow analysis and quantitative analysis of the ability to suppress T cells proliferation when M-MDSCs were treated with 0, 5 and 10 μM STAT3 inhibitor WP1066 for 24 h. (B) p-SATA3 positive cells and (C) PD-L1 positive cells were determined by flow cytometry and quantitative analysis. (D) Secretion of IFN-γ on treated M-MDSCs by ELISA. *P<0.05, **P<0.001, ***P<0.0001. p-, phosphorylated; PD-L, programmed death ligand; M-MDSCs monocytic myeloid-derived suppressor cells.

Last, the percentage of p-STAT3 and PD-L1 positive cells both reached ~90% (Fig. 2E). As shown in Fig. 2D, the level of IFN-γ was significantly decreased in suppressed T cells.

WP1066 treatment leads to downregulation of p-STAT3 and PD-L1. As an important component of the immunosuppressive microenvironment of solid tumors, MDSCs have been extensively studied as therapeutic targets (31). WP1066 is a mature and widely used inhibitor of JAK and STAT3 signaling pathways. However, there are no reports of WP1066 targeting MDSCs. *In vitro* generated MDSCs here were treated with dimethyl sulfoxide (DMSO) plus 0, 5 and 10 μM WP1066 for 24 h to evaluate the inhibitory effect of WP1066 on MDSCs. As shown in Fig. 3A, MDSCs treated with 10 μM

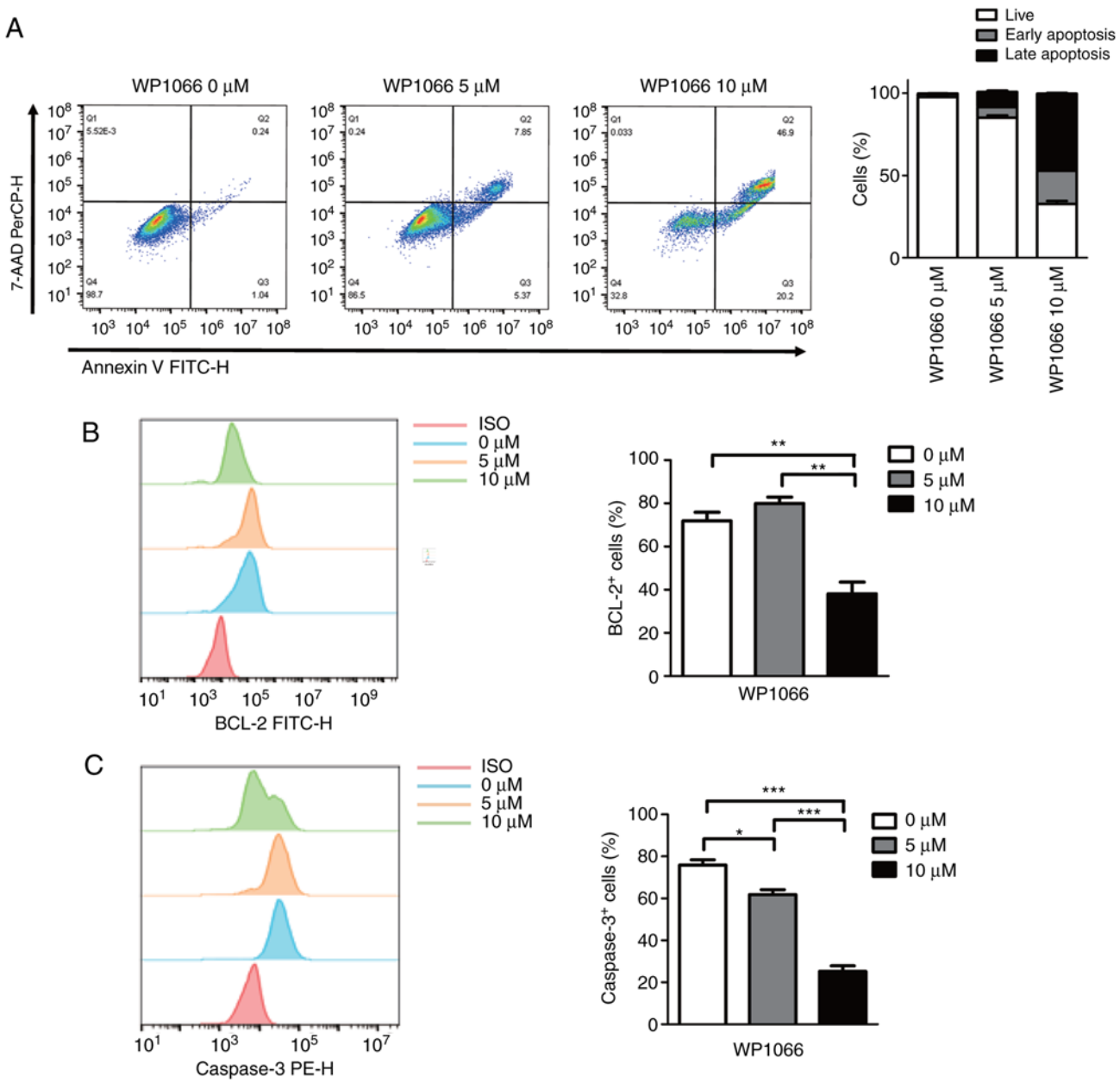

Figure 4. WP1066 treatment leads to upregulation of MDSCs apoptosis and downregulation of apoptosis-related protein. Detection of toxicity of WP1066 on induced M-MDSCs with 0, 5 and 10 μM for 24 h determined by (A) apoptosis analysis of FITC/Annexin V and PerCP/7-AAD, (B) apoptosis relative protein Bcl-2 positive cells and (C) apoptosis relative protein Caspase3 positive cells. *P<0.05, **P<0.001, ***P<0.0001. MDSCs, myeloid-derived suppressor cells.

WP1066 revealed more effectiveness compared with 0 and 5 μM WP1066 in the proliferation of T cells. Similarly, the expression of p-STAT3 (Fig. 3B) and PD-L1 (Fig. 3C) were significantly reduced after 10 μM WP1066 treatment. Finally, with the high-intensity inhibitory effect of WP1066 on M-MDSC cells, the ability of T cells to release IFN-γ was also effectively restored, as shown in Fig. 3D.

WP1066 treatment leads to upregulation of MDSCs apoptosis. In addition to reducing the ability of MDSCs to inhibit T cell proliferation, WP1066 treatment also resulted in an upregulation of cell apoptosis in MDSCs. As shown in Fig. 4A, induced MDSCs treated with 5 μM WP1066 revealed almost the same level of upregulation of early apoptosis and late apoptosis after 24 h of WP1066 treatment, whereas MDSCs treated with 10 μM WP1066 showed more cells with late apoptosis than early apoptosis. Despite the detection of cell viability, classical proteins associated with cell death such as Bcl-2 and Caspase3 were also examined. As shown in Fig. 4B, 5 μM WP1066 did not affect Bcl-2 protein expression in the resulting MDSCs, however, 10 μM WP1066 showed a significant reduction of Bcl-2^{+} cells. Similarly, induced MDSCs treated with 10 μM WP1066 showed more decrease in Caspase3^{+} cells implying more late apoptosis or dead cells (Fig. 4C).

Discussion

The present study established a simple *in vitro* model to generate MDSCs from monocytes isolated from fresh PBMCs by plastic adhesion isolation. Plastic adhesion isolation is a simple and

inexpensive widely used technique for the isolation of human monocytes from PBMCs. Evidently, compared with monocytes isolated by magnetic beads or flow sorting, the yield of adherence monocytes was significantly lower and mixed with a high proportion of lymphocytes. However, only M-MDSCs-like cells were successfully generated from adherence monocytes by co-treatment with IL6 and GM-CSF for 7 days similar to $CD11b^{+}CD14^{+}CD15^{-}CD33^{+}HLA\text{-}DR^{-/low}$ cells. However, it is not claimed to be the best model to generate MDSCs from human bone marrow or PBMCs. Nevertheless, it is suggested that this model will significantly remove the barriers of research funding and high-tech equipment and allow more researchers to study MDSCs-related problems. In addition, it is hypothesized that the feasibility of this technique in diagnosis aspects is not high because diagnosis requires reliable results and high reproducibility. Although this method is the simplest and cheapest method to obtain monocytes, the reliability and consistency of the conclusions using this method are poor and therefore is not suitable for diagnostic applications.

A limitation of the present study is that it only focused on the most commonly used combination of IL6 and GM-CSF to induce MDSCs with greater inhibitory capacity. Further studies will investigate whether MDSCs can be induced from adherence monocytes with the treatment of other different combinations of cytokines or conditional medium of human cell lines. Based on CD14 and CD16 expression, monocytes could be further divided into three main subsets (32), therefore, another limitation of the present study is that it did not explore the proportion of each subset in adherent monocytes.

The first notable phenomenon is that the presence of no-monocytes in the process of early induction did not affect the successful induction of final MDSCs. It was hypothesized that the powerful function of the cytokine combination of IL6 and GM-CSF masked the influence of other lymphocytes early in the process. As in other studies, the STAT3 signaling pathway was activated in MDSCs induced by IL6/GM-CSF, but the characteristics, phenotype and the mechanisms by which MDSCs inhibited T cell proliferation were different. For example, in Casacuberta-Serra *et al* (33), MDSCs express low levels of CD14, but high PD-L1 expression. Bian *et al* (34), show that arginase-1 is neither inherently expressed in MDSC nor required for MDSC-mediated inhibition. Zhan *et al* (35), reveal that the suppressive function of CD33+HLA-DRlow MDSCs is dependent on the programmed death ligand-1/programmed death ligand-2 pathway. However, the IL6/GM-CSF induced MDSCs in the present study lacked ARG1 and NOX2 expression but upregulated VEGF and PD-L1 expression, suggesting that this model is not a classic MDSCs that suppressed T cells proliferation through L-arginine depletion or RNS production. Furthermore, the expression of PD-L1 was upregulated to suppress T cell proliferation. Therefore, this model may be used for therapeutic targets of PD-L1 on MDSCs, but not for other conventional mechanisms of intracellular regulatory molecules in MDSCs isolated from cancer patients.

STAT3 activation is involved in the generation and function of MDSCs and has been identified as a promising therapeutic target for anticancer drugs (36). The present study demonstrated that the STAT3 inhibitor WP1066 had the potential to reduce the level of immunosuppression and upregulate cell apoptosis in MDSCs. It was observed that MDSCs treated with 10 μM WP1066 for 24 h significantly reduced p-STAT3 levels and PD-L1 expression, suggesting that WP1066 could directly inhibit the function of MDSCs. Furthermore, downregulation of Bcl-2 and Caspase3 in MDSCs indicated that WP1066 could promote MDSCs apoptosis to change the tumor microenvironment.

Acknowledgements

Not applicable.

Funding

The present study was supported by the Department of Science and Technology of Hubei Province (project number 2020BCB048) and Hubei Province Technology Innovation Special Major Project (project number 2019ACA168).

Availability of data and materials

The datasets used and/or analyzed during the current study are available from the corresponding author on reasonable request.

Authors' contributions

XL and TZ participated in research design. HH, YX, QY and TL performed the experiments, analyzed the data and were major contributors in writing the manuscript. LG provided technical guidance and participated in data acquisition and analysis. HH and YX confirm the authenticity of all the raw data. All the authors read and approved the final version of the manuscript.

Ethics approval and consent to participate

The present study was approved by the Ethics Committee of the Affiliated Tianyou Hospital, College of Life and Health Sciences, Wuhan University of Science and Technology. Each patient involved in the study was asked to sign a written informed consent form and agreed to the use of their samples in scientific research.

Patient consent for publication

Not applicable.

Competing interests

The authors declare that they have no competing interests.

References

1. Kumar V, Patel S, Tcyganov E and Gabrilovich DI: The nature of myeloid-derived suppressor cells in the tumor microenvironment. Trends Immunol 37: 208-220, 2016.
2. Gabrilovich DI: Myeloid-derived suppressor cells. Cancer Immunol Res 5: 3-8, 2017.
3. Li K, Shi H, Zhang B, Ou X, Ma Q, Chen Y, Shu P, Li D and Wang Y: Myeloid-derived suppressor cells as immunosuppressive regulators and therapeutic targets in cancer. Signal Transduct Target Ther 6: 362, 2021.

4. Huang B, Pan PY, Li Q, Sato AI, Levy DE, Bromberg J, Divino CM and Chen SH: Gr-1+CD115+ immature myeloid suppressor cells mediate the development of tumor-induced T regulatory cells and T-cell anergy in tumor-bearing host. Cancer Res 66: 1123-1131, 2006.
5. Lee CR, Kwak Y, Yang T, Han JH, Park SH, Ye MB, Lee W, Sim KY, Kang JA, Kim YC, *et al*: Myeloid-derived suppressor cells are controlled by regulatory T cells via TGF-β during murine colitis. Cell Rep 17: 3219-3232, 2016.
6. Chen JY, Lai YS, Chu PY, Chan SH, Wang LH and Hung WC: Cancer-derived VEGF-C increases chemokine production in lymphatic endothelial cells to promote CXCR2-dependent cancer invasion and MDSC recruitment. Cancers (Basel) 11: 1120, 2019.
7. Yan HH, Pickup M, Pang Y, Gorska AE, Li Z, Chytil A, Geng Y, Gray JW, Moses HL and Yang L: Gr-1+CD11b+ myeloid cells tip the balance of immune protection to tumor promotion in the premetastatic lung. Cancer Res 70: 6139-6149, 2010.
8. Kusmartsev S, Nefedova Y, Yoder D and Gabrilovich DI: Antigen-specific inhibition of CD8+ T cell response by immature myeloid cells in cancer is mediated by reactive oxygen species. J Immunol 172: 989-999, 2004.
9. Ochoa AC, Zea AH, Hernandez C and Rodriguez PC: Arginase, prostaglandins, and myeloid-derived suppressor cells in renal cell carcinoma. Clin Cancer Res 13: 721s-726s, 2007.
10. Almand B, Clark JI, Nikitina E, van Beynen J, English NR, Knight SC, Carbone DP and Gabrilovich DI: Increased production of immature myeloid cells in cancer patients: A mechanism of immunosuppression in cancer. J Immunol 166: 678-689, 2001.
11. Mirza N, Fishman M, Fricke I, Dunn M, Neuger AM, Frost TJ, Lush RM, Antonia S and Gabrilovich DI: All-trans-retinoic acid improves differentiation of myeloid cells and immune response in cancer patients. Cancer Res 66: 9299-9307, 2006.
12. Alshetaiwi H, Pervolarakis N, McIntyre LL, Ma D, Nguyen Q, Rath JA, Nee K, Hernandez G, Evans K, Torosian L, *et al*: Defining the emergence of myeloid-derived suppressor cells in breast cancer using single-cell transcriptomics. Sci Immunol 5: eaay6017, 2020.
13. Shou D, Wen L, Song Z, Yin J, Sun Q and Gong W: Suppressive role of myeloid-derived suppressor cells (MDSCs) in the microenvironment of breast cancer and targeted immunotherapies. Oncotarget 7: 64505-64511, 2016.
14. Baert T, Vankerckhoven A, Riva M, Van Hoylandt A, Thirion G, Holger G, Mathivet T, Vergote I and Coosemans A: Myeloid derived suppressor cells: Key drivers of immunosuppression in ovarian cancer. Front Immunol 10: 1273, 2019.
15. Taki M, Abiko K, Baba T, Hamanishi J, Yamaguchi K, Murakami R, Yamanoi K, Horikawa N, Hosoe Y, Nakamura E, *et al*: Snail promotes ovarian cancer progression by recruiting myeloid-derived suppressor cells via CXCR2 ligand upregulation. Nat Commun 9: 1685, 2018.
16. Filipazzi P, Valenti R, Huber V, Pilla L, Canese P, Iero M, Castelli C, Mariani L, Parmiani G and Rivoltini L: Identification of a new subset of myeloid suppressor cells in peripheral blood of melanoma patients with modulation by a granulocyte-macrophage colony-stimulation factor-based antitumor vaccine. J Clin Oncol 25: 2546-2553, 2007.
17. Pandit R, Lathers DM, Beal NM, Garrity T and Young MR: CD34+ immune suppressive cells in the peripheral blood of patients with head and neck cancer. Ann Otol Rhinol Laryngol 109: 749-754, 2000.
18. Lathers DM, Achille N, Kolesiak K, Hulett K, Sparano A, Petruzzelli GJ and Young MR: Increased levels of immune inhibitory CD34+ progenitor cells in the peripheral blood of patients with node positive head and neck squamous cell carcinomas and the ability of these CD34+ cells to differentiate into immune stimulatory dendritic cells. Otolaryngol Head Neck Surg 125: 205-212, 2001.
19. Suzuki E, Kapoor V, Jassar AS, Kaiser LR and Albelda SM: Gemcitabine selectively eliminates splenic Gr-1+/CD11b+ myeloid suppressor cells in tumor-bearing animals and enhances antitumor immune activity. Clin Cancer Res 11: 6713-6721, 2005.
20. Blattner C, Fleming V, Weber R, Himmelhan B, Altevogt P, Gebhardt C, Schulze TJ, Razon H, Hawila E, Wildbaum G, *et al*: CCR5^{+} myeloid-derived suppressor cells are enriched and activated in melanoma lesions. Cancer Res 78: 157-167, 2018.
21. Lin S, Wang J, Wang L, Wen J, Guo Y, Qiao W, Zhou J, Xu G and Zhi F: Phosphodiesterase-5 inhibition suppresses colonic inflammation-induced tumorigenesis via blocking the recruitment of MDSC. Am J Cancer Res 7: 41-52, 2017.
22. Kim K, Skora AD, Li Z, Liu Q, Tam AJ, Blosser RL, Diaz LA Jr, Papadopoulos N, Kinzler KW, Vogelstein B and Zhou S: Eradication of metastatic mouse cancers resistant to immune checkpoint blockade by suppression of myeloid-derived cells. Proc Natl Acad Sci USA 111: 11774-11779, 2014.
23. Steele CW, Karim SA, Leach JDG, Bailey P, Upstill-Goddard R, Rishi L, Foth M, Bryson S, McDaid K, Wilson Z, *et al*: CXCR2 inhibition profoundly suppresses metastases and augments immunotherapy in pancreatic ductal adenocarcinoma. Cancer Cell 29: 832-845, 2016.
24. Sun L, Clavijo PE, Robbins Y, Patel P, Friedman J, Greene S, Das R, Silvin C, Van Waes C, Horn LA, *et al*: Inhibiting myeloid-derived suppressor cell trafficking enhances T cell immunotherapy. JCI Insight 4: e126853, 2019.
25. Youn JI, Collazo M, Shalova IN, Biswas SK and Gabrilovich DI: Characterization of the nature of granulocytic myeloid-derived suppressor cells in tumor-bearing mice. J Leukoc Biol 91: 167-181, 2012.
26. Dufait I, Schwarze JK, Liechtenstein T, Leonard W, Jiang H, Escors D, De Ridder M and Breckpot K: Ex vivo generation of myeloid-derived suppressor cells that model the tumor immunosuppressive environment in colorectal cancer. Oncotarget 6: 12369-12382, 2015.
27. Schröder M, Loos S, Naumann SK, Bachran C, Krötschel M, Umansky V, Helming L and Swee LK: Identification of inhibitors of myeloid-derived suppressor cells activity through phenotypic chemical screening. Oncoimmunology 6: e1258503, 2016.
28. Marigo I, Bosio E, Solito S, Mesa C, Fernandez A, Dolcetti L, Ugel S, Sonda N, Bicciato S, Falisi E, *et al*: Tumor-induced tolerance and immune suppression depend on the C/EBPbeta transcription factor. Immunity 32: 790-802, 2010.
29. Lechner MG, Megiel C, Russell SM, Bingham B, Arger N, Woo T and Epstein AL: Functional characterization of human Cd33+ and Cd11b+ myeloid-derived suppressor cell subsets induced from peripheral blood mononuclear cells co-cultured with a diverse set of human tumor cell lines. J Transl Med 9: 90, 2011.
30. Zhang Y, Wilt E and Lu X: Human isogenic cell line models for neutrophils and myeloid-derived suppressor cells. Int J Mol Sci 21: 7709, 2020.
31. Fultang L, Panetti S, Ng M, Collins P, Graef S, Rizkalla N, Booth S, Lenton R, Noyvert B, Shannon-Lowe C, *et al*: MDSC targeting with gemtuzumab ozogamicin restores T cell immunity and immunotherapy against cancers. EBioMedicine 47: 235-246, 2019.
32. Sheng Y, Duan X, Liu Y, Li F, Ma S, Shang X, Wang X, Liu Y, Xue R and Qin Z: Tie2-expressing monocytes/macrophages promote cerebral revascularization in peri-infarct lesions upon ischemic insult. Signal Transduct Target Ther 6: 295, 2021.
33. Casacuberta-Serra S, Parés M, Golbano A, Coves E, Espejo C and Barquinero J: Myeloid-derived suppressor cells can be efficiently generated from human hematopoietic progenitors and peripheral blood monocytes. Immunol Cell Biol 95: 538-548, 2017.
34. Bian Z, Abdelaal AM, Shi L, Liang H, Xiong L, Kidder K, Venkataramani M, Culpepper C, Zen K and Liu Y: Arginase-1 is neither constitutively expressed in nor required for myeloid-derived suppressor cell-mediated inhibition of T-cell proliferation. Eur J Immunol 48: 1046-1058, 2018.
35. Zhan X, Hu S, Wu Y, Li M, Liu T, Ming S, Wu M, Liu M and Huang X: IFN-γ decreased the suppressive function of CD33^{+}HLA-DR^{low} myeloid cells through down-regulation of PD-1/PD-L2 signaling pathway. Mol Immunol 94: 107-120, 2018.
36. Weber R, Riester Z, Hüser L, Sticht C, Siebenmorgen A, Groth C, Hu X, Altevogt P, Utikal JS and Umansky V: IL-6 regulates CCR5 expression and immunosuppressive capacity of MDSC in murine melanoma. J Immunother Cancer 8: e000949, 2020.